Biochimica et Biophysica Acta 1797 (2010) 1034–1044

Contents lists available at ScienceDirect

Biochimica et Biophysica Acta

journal homepage: www.elsevier.com/locate/bbabio

Review

Detection and manipulation of mitochondrial reactive oxygen species in mammalian cells

Marleen Forkink [a], Jan A.M. Smeitink [b], Roland Brock [a], Peter H.G.M. Willems [a], Werner J.H. Koopman [a,c,*]

[a] Department of Biochemistry, Nijmegen Centre for Molecular Life Sciences, Radboud University Nijmegen Medical Centre, Nijmegen, The Netherlands
[b] Department of Pediatrics, Nijmegen Centre for Mitochondrial Disorders, Radboud University Nijmegen Medical Centre, Nijmegen, The Netherlands
[c] Microscopical Imaging of the Cell, Department of Cell Biology, Nijmegen Centre for Molecular Life Sciences, Radboud University Nijmegen Medical Centre, Nijmegen, The Netherlands

ARTICLE INFO

Article history:
Received 12 November 2009
Received in revised form 13 January 2010
Accepted 18 January 2010
Available online 25 January 2010

Keywords:
Hydroethidine
Redox-sensitive GFP
cpYFP
Lipid peroxidation
MitoQ

ABSTRACT

Reactive oxygen species (ROS) are formed upon incomplete reduction of molecular oxygen (O_2) as an inevitable consequence of mitochondrial metabolism. Because ROS can damage biomolecules, cells contain elaborate antioxidant defense systems to prevent oxidative stress. In addition to their damaging effect, ROS can also operate as intracellular signaling molecules. Given the fact that mitochondrial ROS appear to be only generated at specific sites and that particular ROS species display a unique chemistry and have specific molecular targets, mitochondria-derived ROS might constitute local regulatory signals. The latter would allow individual mitochondria to auto-regulate their metabolism, shape and motility, enabling them to respond autonomously to the metabolic requirements of the cell. In this review we first summarize how mitochondrial ROS can be generated and removed in the living cell. Then we discuss experimental strategies for (local) detection of ROS by combining chemical or proteinaceous reporter molecules with quantitative live cell microscopy. Finally, approaches involving targeted pro- and antioxidants are presented, which allow the local manipulation of ROS levels.

1. Introduction

Reactive oxygen species (ROS) are partially reduced derivatives of molecular oxygen (O_2) that can react with many cellular constituents including lipids, proteins and DNA. Depending on the type of cell and its metabolic state, mitochondria can represent a substantial source of ROS within healthy living cells as an unavoidable consequence of metabolism. Important sources of mitochondrial ROS include complex I (CI) of the electron transport chain (ETC) and the tricarboxylic acid (TCA) cycle enzyme α-ketoglutarate dehydrogenase (α-KGDH) [1,2]. Both CI- and α-KGDH generate ROS in the form of superoxide ($O_2^{\bullet -}$), which can be subsequently converted into other ROS including hydrogen peroxide (H_2O_2). Oxidative stress occurs when mitochondrial ROS production exceeds the capacity of the cell's antioxidant systems. In addition to this toxic role, when produced at low levels mitochondrial ROS and its downstream products might also operate as intracellular signaling molecules [3–8]. A signaling function is already well established for reactive nitrogen species (RNS) like nitric oxide as reviewed elsewhere (*e.g.* [9]). Up to now, ROS-dependent signaling has mainly been studied using exogenous ROS generating systems that increase ROS throughout the cell ('global' ROS). However, when produced within living cells the lifetime of a certain ROS limits the distance it can diffuse and thereby its radius of action. This means that the direct reaction of a short-lived ROS like $O_2^{\bullet -}$ *in situ* is likely restricted to a small sub-cellular volume surrounding the site of its generation ('local' ROS) whereas ROS with a longer half-life like H_2O_2 might be more suited for global signaling [6,8,10–13]. Therefore, when endogenously produced at low levels during non-pathological conditions, it is likely that primary ROS predominantly affect closely apposed targets and signaling by these ROS should be highly compartmentalized and local. Proper investigation of this mechanism requires quantitative experimental techniques allowing the local detection and manipulation of ROS and its downstream effects in the living cell. An in-depth discussion of the mechanisms involved in mitochondrial ROS generation and removal falls outside the scope of this review and is presented elsewhere (*e.g.* [5,7,8,14,15]). Therefore we only provide a brief overview about this subject (Sections 2 and 3) followed by a more extensive treatment of experimental strategies for live cell detection and exogenous manipulation of cellular and mitochondrial ROS (Section 4).

Abbreviations: α-KGDH, α-ketoglutarate dehydrogenase; MIM, mitochondrial inner membrane; MOM, mitochondrial outer membrane; RET, reverse electron transfer; ROI, region of interest; $t_{1/2}$, half-life; TPP^+, triphenylphosphonium

* Corresponding author. 286 Biochemistry, Nijmegen Centre for Molecular Life Sciences, Radboud University Nijmegen Medical Centre, P.O. Box 9101, NL-6500 HB Nijmegen, The Netherlands. Tel.: +31 24 3614589; fax: +31 24 3616413.
E-mail address: w.koopman@ncmls.ru.nl (W.J.H. Koopman).
URL: http://ncmd.igmd.nl/page/120/mitochondrial-dynamics.html (W.J.H. Koopman).

0005-2728/$ – see front matter © 2010 Elsevier B.V. All rights reserved.
doi:10.1016/j.bbabio.2010.01.022

2. Sources of mitochondrial ROS

2.1. Types of ROS

The primary ROS, $O_2^{\bullet -}$, is formed by the one-electron reduction of O_2. The latter readily penetrates cells because of its ability to dissolve in the hydrocarbon core of cell membranes. In fact, O_2 was classified as a fat-soluble molecule, as demonstrated by its olive oil/water partition coefficient of 4.4 at 25 °C (see [16] and the references therein). In mitochondria, $O_2^{\bullet -}$ formation is thermodynamically favorable because the reduction potential is high in this compartment ($E_h = 68$ mV), even at low [O_2] (*i.e.* 1 μM) and high [$O_2^{\bullet -}$] (200 pM; [15]). The concentration of $O_2^{\bullet -}$ in the mitochondrial matrix generally is kept low because of the action of manganese superoxide dismutase (MnSOD or SOD2), which converts $O_2^{\bullet -}$ into hydrogen peroxide (H_2O_2). The latter ROS is able to leave the mitochondrion and, when produced in excessive amounts, can also reach the extracellular space [6].

The hydroxyl radical ($OH^{\bullet}$) is another important member of the ROS family, which can be formed under conditions of oxidative stress when high concentrations of $O_2^{\bullet -}$ and/or H_2O_2 are present. In this situation, $O_2^{\bullet -}$ can stimulate H_2O_2 formation and the release of Fe^{2+} from iron–sulphur (FeS)-containing proteins like CI or the TCA cycle enzyme aconitase. Subsequently, the generated Fe^{2+} and H_2O_2 can react to form $OH^{\bullet}$ by the Fenton reaction. The $OH^{\bullet}$ radical is highly reactive, as reflected by its half-life ($t_{1/2}$) of approximately 10^{-9} s, and therefore reacts very close to its site of formation [5]. In comparison, $O_2^{\bullet -}$ and H_2O_2 display much larger $t_{1/2}$ values of 10^{-6} s and 10^{-5} s, respectively [12]. The range of action of each ROS is co-determined by their free aqueous diffusion distance, which appears to have an upper limit of 0.16 μm for $O_2^{\bullet -}$ and 0.23–0.46 μm for H_2O_2 [8]. In the mitochondrion, this distance is likely lowered by the action of ROS scavengers like MnSOD, ROS reactivity with nearby (bio)molecules and the viscosity of the mitochondrial matrix, which is somewhat higher than water. Also singlet oxygen ($^1O_2$) is a member of the ROS family capable of biomolecule oxidation. In contrast to $O_2^{\bullet -}$, H_2O_2 and $OH^{\bullet}$, $^1O_2$ can be formed when endogenous or exogenous photosensitizers absorb light of the appropriate wavelength in the presence of oxygen [10]. Light-induced $^1O_2$ formation can artificially stimulate the oxidation of ROS-reporting sensor molecules (Section 4.1.1) and has been used to locally increase ROS levels (Section 4.2.1).

2.2. Origins of mitochondrial ROS

Most mitochondrial activities, including ATP generation, organelle fusion, protein import and metabolite/ion exchange depend on a proper proton gradient across the MIM. This gradient generates an inward proton-motive force (PMF), which is maintained by the action of 4 ETC complexes (CI–CIV). The PMF consists of both a potential difference ($\Delta\psi$) and a proton gradient (ΔpH), and is used by the F_0F_1-ATP synthetase (CV) to convert ADP into ATP. Together, CI–CV constitute the oxidative phosphorylation (OXPHOS) system. Over the years, several OXPHOS complexes were implicated as relevant sources of ROS. For instance, ROS levels dose-dependently increased upon acute (10 min) and chronic (72 h) treatment with specific inhibitors of CI (rotenone) and CIII (antimycin A) in human skin fibroblasts. In contrast, CV inhibition by oligomycin did not detectably increase ROS levels in these cells [8].

2.2.1. Complex I

Evidence was provided that CI constitutes a major source of ROS in healthy cells [8,14,15]. It appears that $O_2^{\bullet -}$ is generated at the flavin (FMN) group in the NDUFV1 subunit and/or the ubiquinone (CoQ)-binding site of CI [8,15]. In principle, ROS can also be produced by CI via reverse electron transfer (RET) from CII to CI. RET was observed in isolated mitochondria respiring on the CII substrate succinate and is prevented by inhibition of CI using rotenone [17,18]. However, CI inhibition by rotenone in living cells generally results in higher instead of lower ROS levels [19–22]. This suggests that RET might not significantly contribute to mitochondrial ROS formation in healthy cells, although this likely depends on the cell type, rotenone concentration and incubation time [8].

2.2.2. Complex III

In addition to CI also CIII can generate mitochondrial ROS [23,24]. However, experiments in isolated nerve terminals revealed that only very high levels of CIII inhibition (70–80%) lead to detectable increases in H_2O_2 generation [19]. Similarly, only high-level inhibition of CIV increased H_2O_2 levels. In contrast, a 16% inhibition of CI sufficed to increase H_2O_2 levels, suggesting that during physiological conditions CI is a more important ROS source than CIII and CIV in these cells [14]. In human skin fibroblasts, CIII inhibition with antimycin A acutely increased ROS generation with an EC_{50} value of 2.9 nM [8]. Although CIII activity was not determined, this suggest that CIII might also be a source of ROS when just slightly inhibited, implying that the physiological relevance of CIII-mediated ROS generation is cell type specific.

2.2.3. α-Ketoglutarate dehydrogenase

Also α-ketoglutarate dehydrogenase (α-KGDH) can significantly contribute to mitochondrial ROS production [1,2,14]. α-KGDH catalyzes an important step of the TCA cycle, namely the conversion of α-ketoglutarate, coenzyme A and NAD^+ into succinyl-CoA, NADH and CO_2. Mammalian α-KGDH consists of three enzymes: α-ketoglutarate dehydrogenase (E1), dihydrolipoamide succinyltransferase (E2), and dihydrolipoamide dehydrogenase (E3 or Dld). The latter enzyme also constitutes part of the pyruvate dehydrogenase (PDH) enzyme complex. Evidence was provided that the E3/Dld enzyme can generate $O_2^{\bullet -}$. The E3/Dld enzyme contains a flavin group that normally donates electrons to NAD^+. However, when [NAD^+] is low (*i.e.* when the NADH/NAD^+ ratio is high), electrons can be directly transferred to O_2 to form $O_2^{\bullet -}$. Interestingly, α-KGDH is inhibited by its own product succinyl-CoA, by a high NADH/NAD^+ ratio and by a high dihydrolipoate/lipoate ratio. Conversely, α-KGDH is activated by low concentrations of ionic calcium (Ca^{2+}) and matrix ADP [2,25]. This suggests that the increased ROS levels that are generally observed in rotenone-treated cells, might be (partially) due to stimulation of ROS generation by α-KGDH via the rotenone-induced increase in mitochondrial NADH/NAD^+ ratio.

2.2.4. Other mitochondrial ROS sources

In principle, mitochondrial ROS can also originate from several other mitochondrial sources [8,26–29] including $P66^{Shc}$, amine oxidase and α-glycerophosphate dehydrogenase (α-GPDH). Of these, α-GPDH, located on the outer surface of the MIM, appears to be the most important. In mitochondria from brown adipose tissue (BAT) and *Drosophila*, α-GPDH-mediated electron transport from α-glycerophosphate to coenzyme Q is associated with ROS production (see [15] and the references therein). However, the physiological significance of this process is unclear, as α-GPDH is expressed at relatively low levels in most mammalian tissues, although it may be more important in the brain [26].

3. Removal of mitochondrial ROS

Mitochondrial ROS can induce oxidative stress if it exceeds the capacity of ROS detoxifying systems. Alternatively, 'normal' ROS production can induce oxidative stress under conditions where the antioxidant capacity is reduced. Within the mitochondrial matrix, $O_2^{\bullet -}$ is either spontaneously dismutated into H_2O_2 or via a two-electron reaction catalyzed by the tetrameric MnSOD. Using isolated mitochondria, evidence was provided that cytochrome-*c* (cyt-*c*) can

also be involved in the reduction of $O_2^{\bullet-}$ and is regenerated by the action of cyt-*c* oxidase [30,31]. In the cytosol, $O_2^{\bullet-}$ dismutation is predominantly taken care of by copper–zinc-SOD (CuZnSOD or SOD1), which presence was also demonstrated in the mitochondrial intermembrane space (IMS; [32]). In most mammalian cell types H_2O_2 is primarily broken down by catalases (CATs), glutathione peroxidases (GPx) and peroxiredoxins (Prx; [8,15,33]).

CAT catalyzes the conversion of 2 molecules of H_2O_2 into H_2O and O_2 and is mainly expressed in peroxisomes, whereas mitochondria have very low levels of this enzyme. Therefore, mitochondria appear to be a more important cellular source of H_2O_2 than peroxisomes. In the cytosol and mitochondria GPx-mediated conversion of H_2O_2 into H_2O is directly coupled to the oxidative formation of GSSG from glutathione (GSH). GSH is regenerated from GSSG by the action of glutathione reductase (GR) which requires NADPH.

Another mechanism to convert H_2O_2 into H_2O involves the formation of oxidated Prx, which is converted back again into reduced Prx by the oxidation of thioredoxin-2 (TRx). The latter requires NADPH and the action of thioredoxin reductase-2 (TRxR; [8,15]). Although GPxI is considered to be one of the major contributors to H_2O_2 removal in mitochondria, PrxIII is 30-fold more abundant in mitochondria of HeLa cells [34]. Another Prx isoform (PrxV) is also present in mitochondria and its overexpression protects against oxidative damage [35]. As explained above, excessive $O_2^{\bullet-}$ production can also stimulate $OH^{\bullet}$ formation (for its detoxification, see below). $OH^{\bullet}$ induces the formation of carbon-centered lipid radicals ($L^{\bullet}$) from poly-unsaturated fatty acids (LH). These, in turn, can form lipid peroxyl radicals ($LOO^{\bullet}$), which are readily degraded to malondialdehyde β-hydroxyacrolein (MDA) and 4-hydroxynonenal (4HNE). Formation of MDA and 4HNE is counterbalanced by a cascade of antioxidant redox reactions (for more details: see [5,8,15]).

Glutathione (GSH) is one of the most important non-enzymatic antioxidants which further include ascorbic acid (vitamin C), α-tocopherol (vitamin E), vitamin A and its precursor β-carotene, carotenoids, flavonoids and lipoic acid [5,36]. The ratio of GSH to GSSH is a good determinant of the thiol redox state of the cell, and under normal conditions reduced GSH is the more abundant form in the cytosol, nucleus and mitochondria. Since GSH is synthesized in the cytosol, mitochondria have to import it across the MIM [5]. GSH can act as an antioxidant in several ways, for instance: (i) GSH is a cofactor of GPx (see above), (ii) GSH can directly neutralize $OH^{\bullet}$, and (iii) GSH can regenerate vitamins C and E to their active forms [5]. In cells, the most important vitaminic antioxidant is vitamin E, which is lipid-soluble (octanol/water partition coefficient, Log*P* = 10.7; source: pubchem.ncbi.nlm.nih.gov) and exists in 8 different forms (4 tocopherols and 4 tocotrienols). Of these, α-tocopherol seems to have the highest activity in trapping lipid peroxyl radicals ($LOO^{\bullet}$) and thereby preventing the propagation of lipid peroxidation. α-Tocopherol is present in relatively low concentrations in mitochondria of which 22% resides in the MIM and 78% in the mitochondrial outer membrane (MOM; [37]). In theory, also vitamin C can react with lipid peroxyls in its ascorbate form. However, vitamin C is hydrophilic (Log*P* = −1.8) and therefore unlikely to be involved in the direct prevention of lipid peroxidation. However, vitamin C is capable of recycling vitamin E to its reduced form [38,39]. Finally, also CoQ has been recognized as a lipid-soluble mitochondrial antioxidant. Due to its location in the MIM, CoQ appears to primarily act in the prevention of lipid peroxidation but it is also capable of preventing protein oxidation. When reduced, CoQ can regenerate vitamin E from the α-tocopheroxyl radical [40].

4. Detection and manipulation of mitochondrial ROS

4.1. Detection of mitochondrial ROS

Mitochondrial and cellular functions are intricately linked. Therefore experimental approaches are needed that allow the analysis of ROS generation and ROS-induced signaling and/or stress in living cells. We here discuss fluorescence reporter molecules suited for live cell studies that are compatible with epifluorescence and/or confocal laser scanning microscopy (CLSM). The focus will be mainly on fluorescent ROS probes that we have used for live cell analysis in our laboratory but we also discuss some promising novel ROS reporters. In principle, two types of reporter molecules can be distinguished: (i) chemical reporter molecules, which are loaded into the cell using specific incubation ('loading') protocols, (ii) proteinaceous reporter molecules (*i.e.* proteins) that are introduced into the cell by stable or transient transfection.

4.1.1. Chemical ROS reporters

4.1.1.1. Hydroethidine. $O_2^{\bullet-}$ is the initial ROS produced in mitochondria. Due to the relatively small $t_{1/2}$ of $O_2^{\bullet-}$ and its rapid conversion by SODs, quantitative detection of $O_2^{\bullet-}$ is not trivial. A frequently used chemical reporter for superoxide detection is hydroethidine (HEt) and its mitochondria-targeted variant Mito-HEt (a.k.a. MitoSOX-red), which consists of a HEt molecule linked to a cationic triphenylphosphonium (TPP^+) group [41]. Both HEt and Mito-HEt easily cross phospholipid bilayers. The initial oxidation of non-fluorescent HEt and Mito-HEt appears to involve two steps: (i) generation of a radical ($HE^{\bullet+}$) and (ii) successive oxidative formation of two positively charged fluorescent products: ethidium (Et^+) and 2-hydroxyethidium (2-HO-Et^+; [42]). Importantly, only the formation of 2-HO-Et^+ is specific for $O_2^{\bullet-}$. To discriminate between Et^+ and 2-OH-Et^+ fluorescence in living cells, excitation/emission wavelengths of 396/580 nm (only 2-OH-Et^+) and 510/580 nm (Et^+ and 2-OH-Et^+) can be used [41]. Similar to tetramethylrhodamine (TMRM) or rhodamine-123 (R123), the extent of mitochondrial Mito-HEt accumulation depends on its extracellular concentration, the potential difference across the plasma membrane (ΔV) and $\Delta\psi$ [43]. Because of its positive charge, Mito-HEt preferentially accumulates ~1000 fold within the mitochondrial matrix. This accumulation, together with its rapid rate of reaction with $O_2^{\bullet-}$ ($4{\cdot}10^6\ M^{-1}{\cdot}s^{-1}$) should enable Mito-HEt to compete with MnSOD for $O_2^{\bullet-}$ and allow specific detection of mitochondria-generated $O_2^{\bullet-}$ [41]. Of note, also 2-HO-Et^+ and Et^+ are cations and therefore will accumulate in the mitochondrial matrix (see below). However, in case of HEt the origin of its oxidation is more difficult to establish than for Mito-HEt since HO-Et^+ and/or Et^+ can be formed in, for instance, the cytosol and then move to the mitochondrial matrix.

In a previous study [21], we assessed the localization and intensity of HEt oxidation products in human skin fibroblasts using epifluorescence microscopy. To this end, we used a protocol in which cells were incubated with 10 μM HEt for 10 min at 37 °C to allow HEt oxidation, followed by thoroughly washing the cells to remove excess HEt. To measure fluorescence, cells were illuminated by 490 nm excitation light using a monochromator for 100 ms. During this time period fluorescence emission was directed by a dichroic mirror (525DRLP) through a 565 long pass emission filter (565ALP) onto a CoolSNAP HQ monochrome charge-coupled device (CCD) camera. Image acquisition at 0.2 Hz did not increase the fluorescence signal for at least 10 min [21]. This indicates that excess HEt was effectively removed, fluorescent HEt oxidation products did not leak out of the cell, and photobleaching and/or photoactivation did not occur during this time period. Using the above approach, and considering the *in vitro* spectral properties of Et^+ and 2-OH-Et^+ [42], the contribution of 2-OH-Et^+ to the total fluorescence signal is expected to be ~2-fold higher than that of Et^+. HEt oxidation products were detected in mitochondrial tubules and the nucleus (nucleoli; Fig. 1A). Individual cells always displayed a higher nuclear than mitochondrial fluorescence, compatible with the increased fluorescence quantum yield upon DNA-binding of Et^+ and 2-OH-Et^+ [42] and/or a higher nuclear viscosity. However, both in cells from patients with isolated nDNA-encoded CI deficiency and rotenone-treated fibroblasts, nuclear

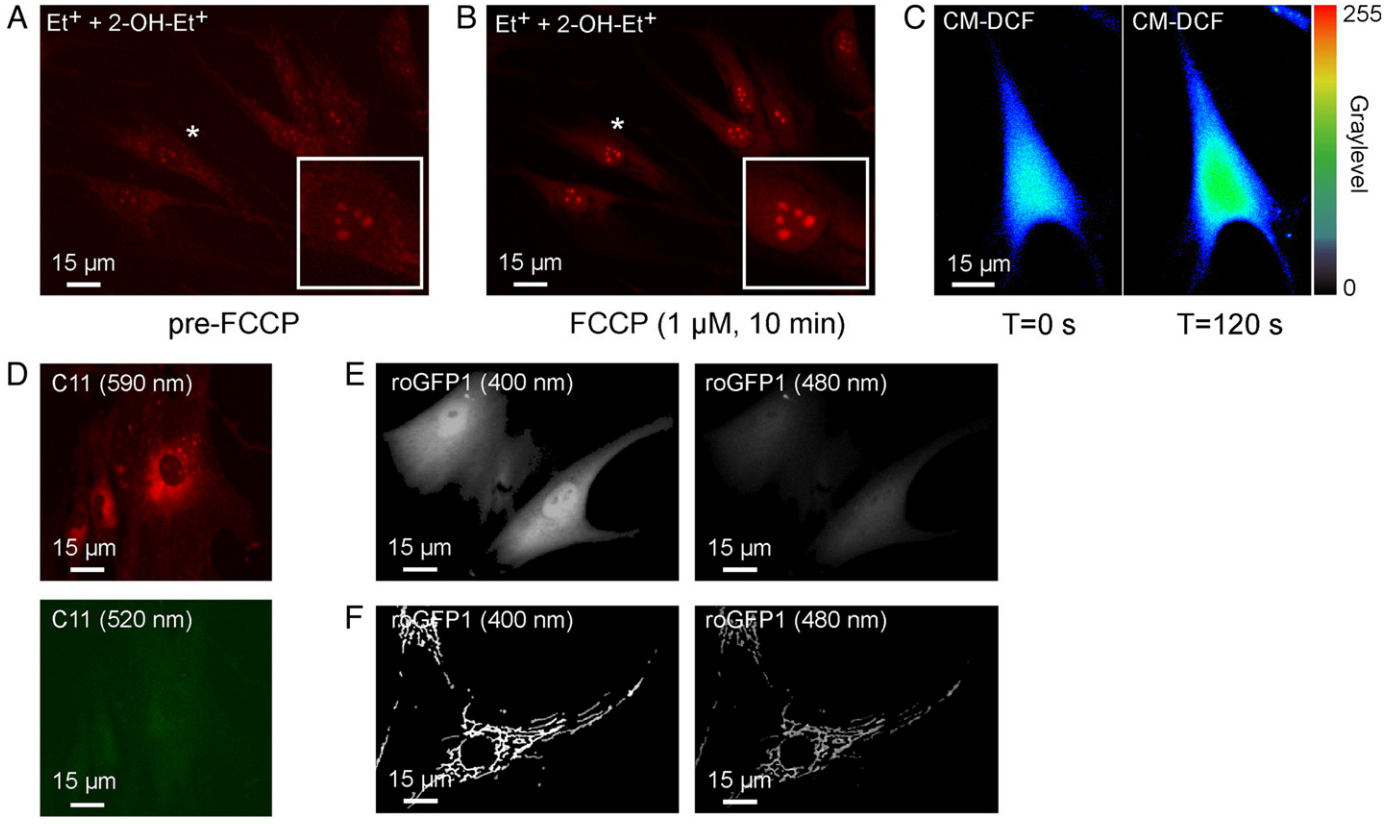

Fig. 1. Quantification of ROS, cellular lipid peroxidation and thiol redox environment in human skin fibroblasts. (A) Typical confocal fluorescence image of human skin fibroblasts incubated with 10 μM hydroethidine (HEt) for 10 min (37 °C). Fluorescence signals arise from the ROS-stimulated formation of ethidium (Et^+) and/or 2-hydroxyethidium (2-HO-Et^+), and were detected in both nucleoli and a widespread network of tubular structures in the cytosolic compartment. The white box depicts a magnified view of the cell marked with an asterisk. (B) Upon addition of the mitochondrial uncoupler carbonylcyanide-*p*-trifluoromethoxy-phenylhydrazone (FCCP; 1 μM), staining of the cytosolic tubular structures was lost and Et^+/2-HO-Et^+ translocated to the nucleus. (C) Typical confocal fluorescence images of a human skin fibroblast pre-stained with 1 μM of 5-(and-6)-chloromethyl-2′,7′-dichlorodihydro-fluorescein diacetate (CM-H2DCFDA) for 10 min (37 °C). Fluorescence arises from the ROS-stimulated formation of CM-DCF, which occurs linearly over time. By measuring the rate of fluorescence increase at different time points, the level of CM-DCF-formation inducing ROS can be determined. (D) Typical confocal fluorescence image of human skin fibroblasts incubated with the fluorescent lipid peroxidation probe C11-BODIPY$^{581/591}$ (4 μM, 30 min, 37 °C). Upon oxidation, the red emitting form of the dye (590 nm) is converted into a green emitting form (520 nm), which results in an increase in green-to-red emission ratio. (E) Typical epifluorescence image of human skin fibroblasts expressing cytosolic roGFP1 (cyt-roGFP1), a fluorescent proteinaceous thiol redox sensor. The latter was expressed using a baculoviral transduction system. The fluorescence emission ratio of roGFP1 after excitation at 400 nm (oxidized state) and 480 nm (reduced state) is a measure of the ambient thiol redox environment. (F) Same as panel E but now for the mitochondrial matrix-targeted variant of roGFP1 (mit-roGFP1). Used fibroblast cell lines: #5120 (panels A,B,C); #5067 (panel E), #5170 (panel F) [76].

and mitochondrial Et^+/2-OH-Et^+ signals increased proportionally [4,21]. This means that either signal can be used to quantify Et^+/2-OH-Et^+ fluorescence. Protonophore-induced dissipation of $\Delta\psi$ induced a rapid decrease in tubular fluorescence and concomitant increase in the nuclear fluorescence signal, indicating translocation of Et^+/2-OH-Et^+ from the mitochondrial to the nuclear compartment (Fig. 1B; [4]). This means that Et^+/2-OH-Et^+ are (partially) retained in the mitochondrial matrix in a $\Delta\psi$-dependent manner. Therefore it is important that when reduced mitochondrial Et^+/2-OH-Et^+ signals are observed, also $\Delta\psi$ is quantified in parallel experiments. An approach allowing proper quantification of $\Delta\psi$ has been described elsewhere [44].

To compare HEt and Mito-HEt, human control fibroblasts were cultured in the presence of vehicle (CT) or rotenone (R; 100 nM) for 72 h. Next, cells were incubated with 10 μM HEt or Mito-HEt for 10 min at 37 °C and images were acquired using illumination times of 100 ms and 500 ms for HEt and Mito-HEt, respectively. We used spectral settings allowing (i) combined detection of Et^+ and 2-OH-Et^+ (490 nm excitation, 580 nm emission) or, (ii) more specifically 2-OH-Et^+ (405 nm excitation, 580 emission) (Fig. 2). Cells stained with HEt or Mito-HEt displayed fluorescence signals in cytosolic tubular structures (*i.e.* mitochondria) as well as in the nucleoli (Fig. 2A). Fluorescence signals obtained with 405 nm excitation were much lower (*i.e.* closer to the background signal) than with 490 nm excitation. This suggests that the extent of $O_2^{\bullet-}$-specific 2-OH-Et^+ formation is overestimated when 490 nm excitation is used. Analysis of a large quantity of cells from multiple experiments revealed an identical rotenone-induced fluorescence increase (to ~220% of CT) for 405 and 490 nm excitation in HEt-stained cells (Fig. 2B; left panel). In case of Mito-HEt, the rotenone-induced fluorescence increase was less (to ~140–175% of CT) than for HEt and significantly lower ($p < 0.001$) for 405 nm excitation than for 490 nm (Fig. 2B; right panel). These results support our above conclusion that a large fraction (~50%) of HEt-detectable ROS in rotenone-treated fibroblasts (using 490 nm excitation) consists of $O_2^{\bullet-}$ originating from mitochondria.

4.1.1.2. CM-H_2DCFDA. The oxidative conversion of non-fluorescent 2′,7′-dichlorodihydrofluorescein (H_2DCF) into fluorescent 2′,7′-dichlorofluorescein (DCF) has been widely applied to measure oxidant levels in living cells. This compound is typically loaded into cells in the form of a membrane-permeant diacetate (DA) ester, which is converted into a membrane impermeant product inside the cell. Still, DCF has been shown to be prone to passive leakage across the plasma membrane which limits the duration of cell observation after loading. Therefore, a DCF variant with chloromethyl groups (CM-H_2DCF) was developed with greatly reduced passive dye leakage (see [45] and the references therein). By attaching esterase-cleavable DA groups to CM-H_2DCF its membrane-permeability was improved. The resulting 5-(and-6)-chloromethyl-2′,7′-dichlorodihydrofluorescein diacetate (CM-H_2DCFDA) is rapidly taken up by cells. Intracellularly, it is converted into non-fluorescent CM-H_2DCF by esterase action and

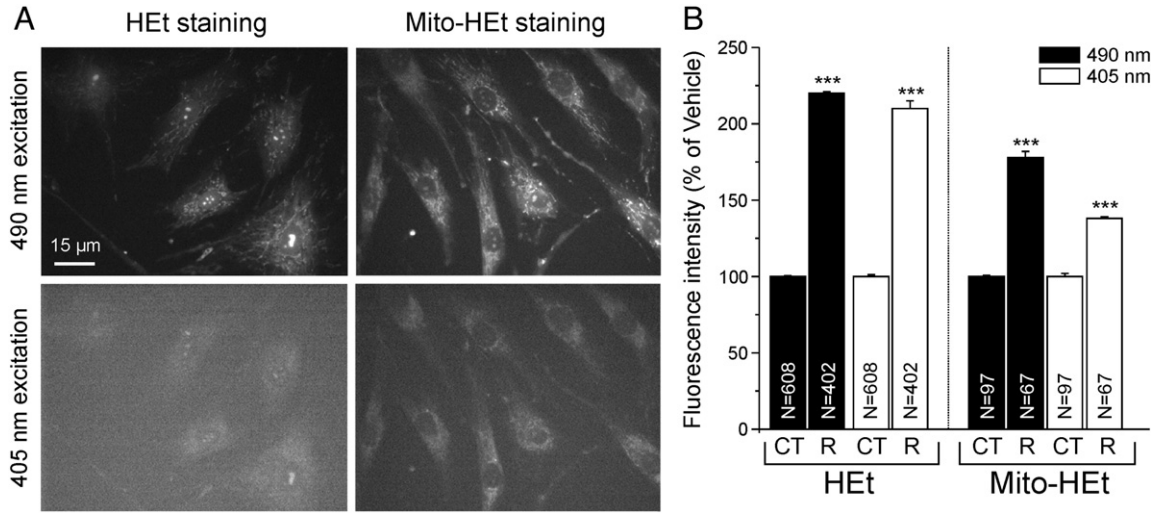

Fig. 2. Comparison of the fluorescence signals of hydroethine (HEt) and mitochondria-targeted HEt (Mito-HEt) in human skin fibroblasts. (A) Typical epifluorescence images of human skin fibroblasts stained with HEt or Mito-HEt. Fluorescence arises from the ROS-stimulated formation of ethidium (Et^+) and/or 2-hydroxyethidium (2-HO-Et^+) and images were acquired to allow combined detection of Et^+ and 2-OH-Et^+ (490 nm excitation) or preferentially 2-OH-Et^+ (405 nm excitation). Individual images in this panel were linearly contrast-stretched for visualization purposes. (B) Effect of rotenone (R) treatment (100 nM, 72 h) on fluorescence signals in cells stained with HEt (left panel) or Mito-HEt (right panel). In this figure, significant differences between vehicle-control (CT) and rotenone-treated cells are marked by *** ($p<0.001$), error bars indicate standard-error of the mean and numerals reflect the number of cells analyzed in at least two independent experiments. Used fibroblast cell line: #5120.

subsequently oxidized by intracellular oxidants into highly fluorescent CM-DCF. The levels of CM-DCF-forming ROS can be reliably determined by measuring the rate of CM-DCF formation (see Fig. 1C; [45,46] and the explanation below).

In human skin fibroblasts acute application of H_2O_2 stimulated CM-DCF formation [45–47]. Interestingly, H_2O_2 but also $O_2^{\bullet-}$, Fe(III), GPx and cyt-*c* were unable to stimulate fluorescent DCF formation from H_2DCF in a cell free system [48]. In contrast, when horseradish peroxidase, Fe(II), CAT, CuZnSOD, xanthine oxidase, $ONOO^-$, or nitric oxide were present DCF formation was stimulated [48–50]. Together, these results are compatible with the idea that intact cells contain catalysts, like transition metal ions, heme peroxidases, and/or CuZnSOD that enable the H_2O_2-induced formation of CM-DCF. In this respect, evidence was provided that H_2O_2 stimulates CM-DCF formation through a peroxide-catalyzed reaction [51]. From a chemical point of view, it was proposed that the reaction mechanism for the formation of CM-DCF from CM-H_2DCF involves two main steps [52]: (i) conversion of CM-H_2DCF into CM-DCFH$^{\bullet}$/CM-DCF$^{\bullet-}$ stimulated by $CO_3^{\bullet-}$, $NO_2^{\bullet}$ and/or peroxidase-like catalysts involving conversion of GS$^{\bullet}$ into GSH, (ii) formation of CM-DCF stimulated by generation of $O_2^{\bullet-}$ from O_2. The mechanism also involves three other (side) reactions: (iii) conversion of CM-DCF into a phenoxyl radical (CM-DCF-O$^{\bullet}$) stimulated by $CO_3^{\bullet-}$, $NO_2^{\bullet}$ and/or peroxidase-like catalysts, (iv) light-induced formation of 'DCF*' and (v) back-conversion of DCF* into CM-DCFH$^{\bullet}$/CM-DCF$^{\bullet-}$ from CM-DCF paralleled by formation of GS$^{\bullet}$ from GSH. Reactions iv and v are compatible with the observation that laser light can stimulate CM-DCF formation (see [45] and references therein). In this sense, evidence has been provided that photo-oxidation of CM-DCF is stimulated by $^1O_2$ generated upon irradiation with laser light with $\lambda > 300$ nm [53]. However, $^1O_2$ is unable to directly enhance CM-DCF formation but induces formation of CM-DCFH$^{\bullet}$/CM-DCF$^{\bullet-}$, possibly via reactions iv and v in the above mechanism. Next, CM-DCFH$^{\bullet}$/CM-DCF$^{\bullet-}$ is then converted into CM-DCF (reaction i) paralleled by formation of $O_2^{\bullet-}$.

Our findings in human skin fibroblasts show that the relative contribution of the photo-oxidation process is minimal at the lowest practical laser intensity of 34 µW (488 nm, measured at the aperture of the objective). To maximize the sensitivity of fluorescence detection at this low laser intensity, we used a 500 nm long pass (LP) instead of a band-pass emission filter. Furthermore, we applied optimal black level and brightness settings, whereas the signal-to-noise ratio was improved by real time image averaging [45]. We further observed that when the above imaging approach was used, CM-DCF fluorescence increased linearly with time during maximally 200 s. This means that during this time the oxidative conversion of CM-H_2DCF to CM-DCF proceeds according to a zero-order reaction, given by: $[\text{CM-DCF}](t) = V_{\text{CM-DCF}} \cdot t + [\text{CM-DCF}]_0$ with $[\text{CM-DCF}](t)$ being the recorded CM-DCF fluorescence signal, $V_{\text{CM-DCF}}$ being the rate of fluorescence increase and $[\text{CM-DCF}]_0$ being the CM-DCF fluorescence signal at the beginning of the recording ($t=0$). From this equation, it follows that $V_{\text{CM-DCF}}$ is independent of [CM-H_2DCF] and therefore solely determined by the steady-state oxidant level [45]. The zero-order model predicts that $V_{\text{CM-DCF}}$ increases as a function of $[\text{CM-DCF}]_0$. Indeed, $V_{\text{CM-DCF}}$ changed proportionally with $[\text{CM-DCF}]_0$ in fibroblasts from healthy volunteers and from patients with isolated CI deficiency [45]. Also in the presence of H_2O_2, $V_{\text{CM-DCF}}$ and $[\text{CM-DCF}]_0$ increased to the same extent. Beyond a measuring time of 200 s, however, the increase in CM-DCF fluorescence became supralinear. This may suggest that CM-DCF, once formed in sufficient quantities, stimulates the conversion of CM-H_2DCF into CM-DCF. Alternatively, cellular oxidant levels might increase upon prolonged laser illumination, thereby accelerating the formation of CM-DCF. Our results demonstrate that normalization of the CM-DCF time trace (*i.e.* dividing by $[\text{CM-DCF}]_0$) is not appropriate, since this would lead to underestimation of $V_{\text{CM-DCF}}$ at higher $[\text{CM-DCF}]_0$.

The lack of specificity of CM-DCF formation makes it difficult to identify the nature of the oxidants detected by the probe [52,54]. Therefore, the formation of CM-DCF in cellular systems can best be considered as a marker of cellular oxidant levels rather than as a direct reporter of a specific ROS/RNS species [45]. In human skin fibroblasts, rotenone-treatment readily increased the rate of Et^+/2-OH-Et^+ formation without affecting the rate of CM-DCF formation [4], suggesting that the formation of Et^+/2-OH-Et^+ and CM-DCF is stimulated by different types of ROS and/or in different cellular compartments. The latter is compatible with the fact that CM-H_2DCF has a very low reactivity towards $O_2^{\bullet-}$ [52].

4.1.1.3. Dihydrorhodamine 123. Dihydrorhodamine 123 (DHR123) is a reduced rhodamine that is unreactive towards $O_2^{\bullet-}$ and H_2O_2 in the absence of catalysts [52]. Fluorescent R123 is directly formed in the

presence of $OH^{\bullet}$, $CO_3^{\bullet-}$, $NO_2^{\bullet}$, hypochlorous acid (HClO), $ONOO^-$, Fe^{2+} and cyt-*c* [52,55]. In this respect, also DHR123 constitutes a marker of overall oxidant levels. In cells, formation of R123 can be monitored using 488 nm excitation light and emission detection >500 nm [21]. Given the cationic nature of R123, it is important to also quantify $\Delta\psi$ in parallel experiments (see above) when a reduced cellular R123 staining is encountered.

4.1.1.4. C11-BODIPY$^{581/591}$. An indirect means to measure mitochondrial ROS production in living cells is through assessing the extent of lipid peroxidation. A suitable reporter molecule for this purpose is the fatty acid analogue C11-BODIPY$^{581/591}$ (Fig. 1D) which is insensitive to $O_2^{\bullet-}$, nitric oxide and hydroperoxides [56]. Upon oxidation, the red emitting reduced form of the dye (595 nm) is converted into a green emitting oxidized form (520 nm), which results in an increase in green-to-red emission ratio [57]. We have quantified lipid peroxidation in human skin fibroblasts by confocal microscopy using an excitation wavelength of 488 nm, a 560DM dichroic mirror and appropriate band-pass filters (535D20 and 580LP; [21]). Upon treatment with rotenone, the green/red C11-BODIPY$^{581/591}$ emission ratio increased 2-fold. However, in the presence of the mitochondria-targeted MIM-embedded antioxidant MitoQ (see Section 4.1.2), rotenone was unable to stimulate C11-BODIPY$^{581/591}$ oxidation. These data demonstrate that lipid peroxidation is stimulated by rotenone and that this effect is completely blocked by MitoQ. Fluorescence recovery after photobleaching (FRAP; [58]) analysis revealed that the laser bleach pulse (488 nm) increased the level of oxidized (green) C11-BODIPY$^{581/591}$ (Fig. 3A). This suggests that high-intensity laser illumination induces oxidation of C11-BODIPY$^{581/591}$ and/or membrane lipids. Next, the FRAP dynamics of the red emitting form and the FLIP (fluorescence loss in photobleaching) dynamics of the green emitting form in a region of interest (ROI) distal to the FRAP region were analyzed (Fig. 3B). This revealed a similar (slow) mobility for the red- and green-emitting forms of C11-BODIPY$^{581/591}$ compatible with their

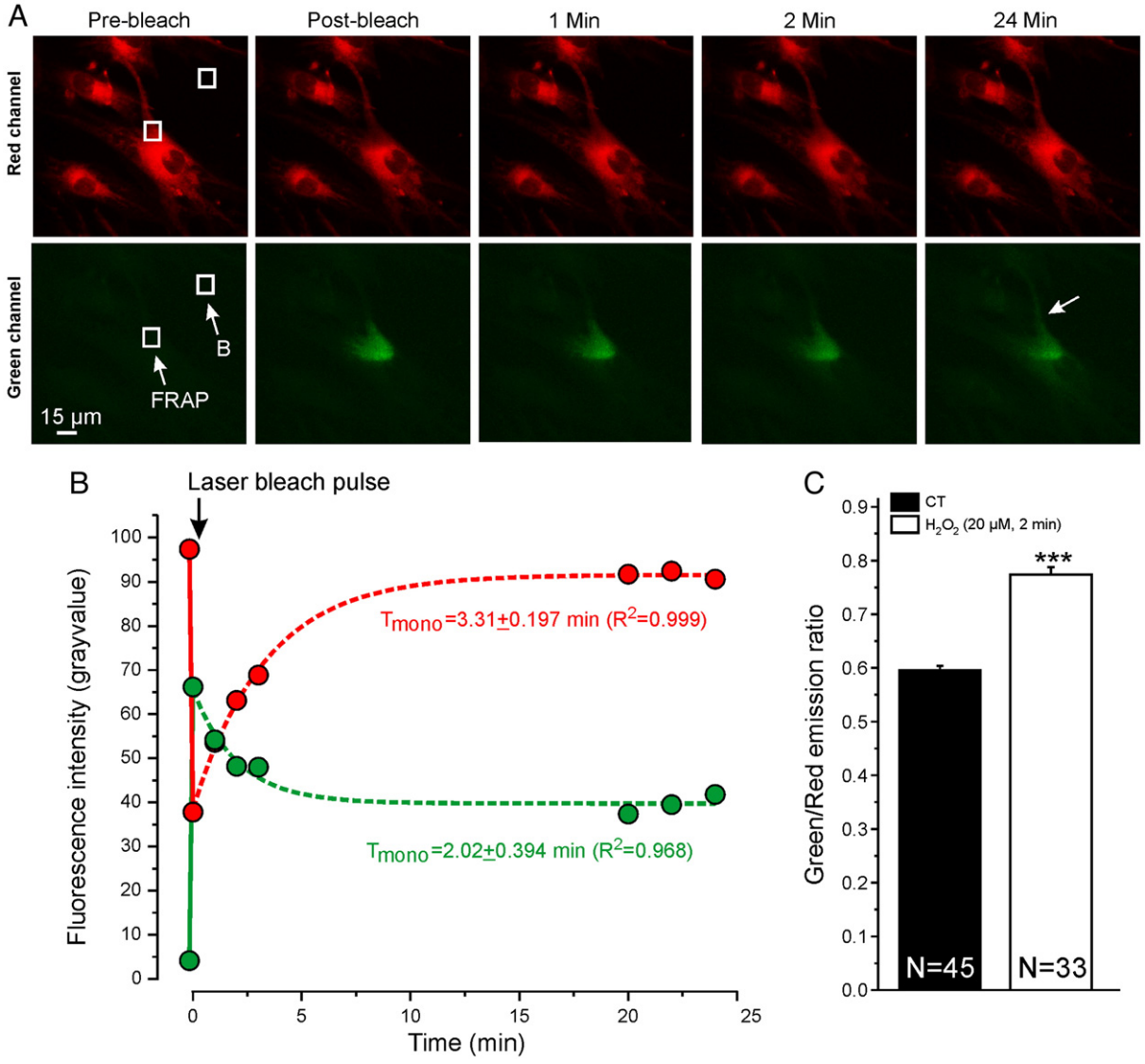

Fig. 3. Properties of the lipid peroxidation sensor C11-BODIPY$^{581/591}$ in human skin fibroblasts. (A) Analysis of the mobility of C11-BODIPY$^{581/591}$ by fluorescence recovery after photobleaching (FRAP) analysis using confocal microscopy. A FRAP and background (B) region of interest (ROI) were defined in the pre-bleach image and fluorescence recovery was measured over time for the red and green emitting forms of C11-BODIPY$^{581/591}$. (B) Oxidation of C11-BODIPY$^{581/591}$ by the laser bleach pulse resulted in a reduction in fluorescence of the red emitting form of the dye (590 nm) and an increase in fluorescence of the green emitting form (520 nm). FRAP kinetics for the red and FLIP (fluorescence loss in photobleaching) kinetics for the green form of C11-BODIPY$^{581/591}$ were similar and yielded a time constant in the range of minutes, compatible with its membrane localization. FRAP and FLIP signals were fitted using a mono-exponential model ($Y = Y_0 + A_1 \cdot e^{-t/Tmono}$). (C) When cells were treated with hydrogen peroxide (H_2O_2), the C11-BODIPY$^{581/591}$ green/red emission ratio was increased, indicative of lipid peroxidation. In this figure, significant differences between vehicle- (CT) and H_2O_2-treated cells are marked by *** ($p<0.001$), error bars indicate standard-error of the mean and numerals reflect the number of cells analyzed in at least two independent experiments. Used fibroblast cell line: #5120 [76].

localization in membranes. When cells were treated with hydrogen peroxide (H_2O_2), the C11-BODIPY$^{581/591}$ green/red emission ratio was increased, indicative of lipid peroxidation (Fig. 3C).

4.1.2. Proteinaceous ROS reporters

Protein-based ROS reporter molecules have the distinct advantage that they can be selectively expressed in different cell compartments (*e.g.* nucleus, ER lumen, mitochondrial matrix, MIM, MOM, golgi lumen, golgi membrane, plasma membrane) by N- or C-terminally fusing them to specific targeting sequences [59]. For mitochondrial matrix expression, the N-terminal targeting sequence of subunit VIII of cytochrome-*c* oxidase (Cox8) is frequently used (MSVLTPLLLRGLTGSARRLPVPRAKIHSLGDP). For several reporter molecules, 2–3 subsequent Cox8 targeting sequences are needed to ensure proper targeting and efficient expression [59–61]. In addition to targeting sequences, proteinaceous reporters can also be fused to specific ROS generating or ROS detoxifying proteins of interest allowing local detection. In the latter case, it should be investigated whether steric hindrance or folding interference between the protein and the reporter molecule is present. To minimize the chance of steric hindrance, a linker between the protein of interest and reporter molecule is generally used. Such a linker should be flexible, soluble, resistant to proteolysis and display no secondary structure or aggregation [62]. In this respect, Miyawaki et al. constructed a series of DNA plasmids that facilitate the fusion of coding sequences for any two protein domains with a DNA linker that encodes a triple repeat of the amino-acid linker Gly-Gly-Gly-Gly-Ser (*i.e.* [$(GGGGS)_3$]; [63]). Below we discuss protein-based reporters for detection of $O_2^{\bullet-}$, H_2O_2 and thiol redox status.

4.1.2.1. cpYFP. Recently, a circularly permuted YFP (cpYFP), previously used as a core component of the ratiometric Ca^{2+} indicator Pericam [64], was presented as a specific reporter of $O_2^{\bullet-}$ [65]. In this study, cpYFP was targeted to the mitochondrial matrix (mt-cpYFP) using the cytochrome-*c* oxidase subunit IV (Cox4) targeting sequence with the aim to measure $O_2^{\bullet-}$ in this compartment. Interestingly, it was observed that the mt-cpYFP fluorescence signal displays transient all or none 'flashes'. However, in a recent comment several points of concern have been raised regarding the $O_2^{\bullet-}$-specificity of cpYFP [66], the most important being that the total removal of O_2 did not completely abolish mt-cpYFP flashes. Moreover, mt-cpYFP flashes were absent in the presence of the CIII-inhibitor antimycin A, which is demonstrated to stimulate $O_2^{\bullet-}$-generation in many different experimental systems. It was proposed that the changes in mt-cpYFP flashes observed in the various experiments might reflect changes in ATP levels, rather than $O_2^{\bullet-}$, and as such are linked to the energization state of mitochondria [66]. The latter explanation might relate to previous findings, revealing that fluctuations in free or Mg^{2+}-bound ATP can affect the signal output of CFP-YFP-based FRET sensors [67]. In this respect it is interesting to note that the HyPer H_2O_2 sensor (see next section), which contains cpYFP, is insensitive to $O_2^{\bullet-}$. Importantly, the fluorescence ratio of cpYFP and Hyper is also pH-dependent. This dependency is similar to that reported for ratiometric Pericam, which exhibited pH-induced changes in fluorescence ratio between pH 6 and pH 10 [64]. Therefore measurements with cpYFP or HyPer should be accompanied by parallel pH quantification [68]. The latter could be carried out using chemical reporters in the cytosol (*e.g.* BCECF, SNARF-1) or mitochondria-targeted protein-based pH sensors like 'pHluorins' [69] or 'pHlameleons' [70]. Taken together, it appears that more experimental data is required to determine the value of cpYFP as a specific $O_2^{\bullet-}$-sensor.

4.1.2.2. HyPer. HyPer is a fluorescent ratiometric ROS sensor in which a cpYFP is inserted into the regulatory domain of the *E. coli* transcription regulator OxyR [68]. OxyR contains an H_2O_2-sensitive domain (amino acids 80–310) and a DNA-binding domain (amino acids 1–79). Upon oxidation by H_2O_2, the reduced form of OxyR is converted into an oxidized DNA-binding form. As a result, dramatic conformational changes occur in the regulatory domain of OxyR [71]. HyPer was generated by inserting cpYFP between residues 205 and 206 of the OxyR regulatory domain. Importantly, cpYFP fluorescence was demonstrated to be very sensitive to conformational changes of an attached protein [64]. HyPer displays two excitation peaks at 420 nm (reduced form) and 500 nm (oxidized form) and a single emission peak at 516 nm. Upon H_2O_2 application, the HyPer fluorescence emission following 420 and 500 nm excitation decreases and increases, respectively. HyPer was rapidly oxidized by submicromolar [H_2O_2] even in highly reducing intracellular environments [71]. Quantitatively, the minimal [H_2O_2] required to induce a detectable change in HyPer fluorescence in mammalian cells was ~5 μM. Importantly, HyPer was demonstrated to be specific for H_2O_2 and did not react with $O_2^{\bullet-}$, GSSG, nitric oxide, and $ONOO^-$ [68], allowing the use of the 500/420 HyPer signal ratio as a measure of [H_2O_2]. As argued in the previous section, HyPer is also pH-sensitive and therefore its use should be accompanied by pH measurements. When targeted to mitochondria (mt-HyPer), local bursts in mt-HyPer ratio were observed during $\Delta\psi$ oscillations in apoptotic HeLa cells [68]. Interestingly, the latter study revealed that H_2O_2 production can be confined to single depolarized mitochondria. This is compatible with the calculated small range of action of this ROS [8] and was proposed to be due to the fast dilution of mitochondria-generated H_2O_2 in the cytosol and/or the action of cytosolic CAT [68]. HyPer was also applied to quantify insulin-induced H_2O_2 generation in myotubes [72], EGF-induced H_2O_2 generation in HeLa cells [71], mitochondrial H_2O_2 production in coronary arterial epithelial cells [73] and H_2O_2-levels in zebra fish [74].

4.1.2.3. roGFPs. Reduction–oxidation-sensitive GFPs (roGFPs) have been generated by substitution of surface-exposed residues of GFP with cysteines in appropriate positions to form disulfide bonds [75]. RoGFPs display two fluorescent excitation maxima whose relative amplitudes depend on the state of oxidation. In cells, the reduced and oxidized forms of roGFP1 are specifically excited at 480 and 400 nm respectively. Fluorescence emission of both roGFP1 forms is detected at 530 nm. This means that the 400/480 ratio of roGFP1 can be used as a measure of roGFP1 oxidation status. In our research [76] we used cytosolic (Fig 1E; cyt-roGFP1) and mitochondria-targeted variants (Fig. 1F; mt-roGFP1) of roGFP1 (*i.e.* GFP with mutations C48S, S147C and Q204C; [77]). Both roGFP1 variants were introduced into human skin fibroblasts by means of baculoviral transfection. To visualize roGFP1-expressing cells we used a similar epifluorescence system as for HEt (see above), with alternating 300 ms excitation at 400 and 480 nm using a monochromator. Fluorescence was detected by guiding the emission light via a dichroic mirror (525DRLP) through a 535 band-pass filter (535DF25) onto the CCD camera. Quantification of cyt-roGFP1 and mt-roGFP1 signals is illustrated in Fig. 4.

In cyt-roGFP1-transfected cells (Fig. 4A), fluorescence in the cytosol (continuous ROIs), nucleus (dotted ROIs) and background fluorescence (ROI marked 'B') were quantified for both wavelengths. The background-corrected individual wavelength signals of roGFP1 (Fig. 4B) were used to calculate the roGFP1 ratio for the different ROIs as a function of time (Fig. 4C). To establish the extent of roGFP1 oxidation, ratios were calibrated by successive addition of 1 mM hydrogen peroxide (H_2O_2) and 10 mM dithiothreitol (DTT) to fully oxidize (100% oxidation) and reduce (0% oxidation) the probe, respectively [75,76]. H_2O_2 gradually increased the fluorescence emission ratio to a maximum reached within 350 s, whereas subsequent addition of DTT rapidly reduced this ratio to below pre-H_2O_2 levels. Higher concentrations of H_2O_2 and DTT caused no further change in fluorescence emission ratio, indicating that the probe was maximally oxidized and reduced, respectively [76]. A similar analysis was carried out with mt-roGFP1 (Fig. 4D–F). No difference was observed between the roGFP1 oxidation status in the nucleus and cytosol of resting cells. However, comparison of Fig. 4C and F reveals that the extent of roGFP1 oxidation

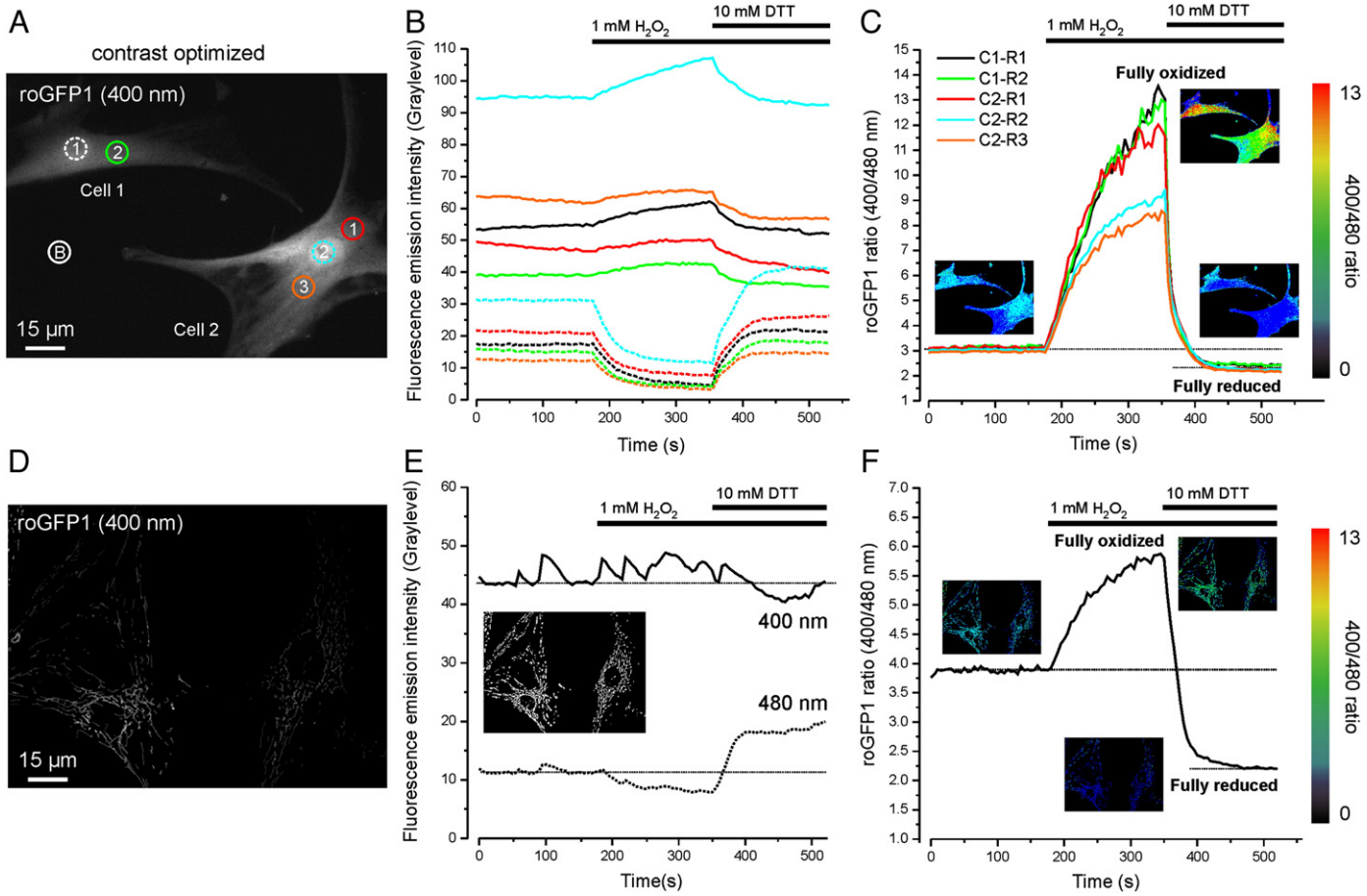

Fig. 4. Use of the proteinaceous thiol redox sensor roGFP1 in human skin fibroblasts. (A) Fluorescence image (400 nm excitation) of a fibroblast transiently expressing the cytosolic variant of roGFP1 (cyt-roGFP1). Circles represent regions of interest (ROIs) used for quantitative measurement of thiol redox state in cell 1 (nucleus: ROI1, cytosol: ROI2) and cell 2 (nucleus: ROI2, cytosol: ROI1, ROI3) and an extracellular region used for background correction (B). Color coding corresponds to the traces in panels B and C. (B) Background-corrected fluorescence signals of the oxidized (400 nm excitation, continuous lines) and reduced forms (480 nm excitation, dotted lines) of cyt-roGFP1 for the ROIs in panel A. The thiol redox status of roGFP1 was calibrated using 1 mM H_2O_2 (fully oxidized) and 10 mM DTT (fully reduced). (C) Cyt-roGFP ratio signal (400/480 nm) calculated from the individual signals in panel B. Images depict the color-coded cyt-roGFP1 ratio in resting cells (scale to the right) and in the fully oxidized and reduced state. (D) Similar to panel A but now for the mitochondria-targeted variant of roGFP1 (mit-roGFP1). (E) Average background-corrected mitochondrial fluorescence signals of the oxidized (400 nm excitation, continuous lines) and reduced forms (480 nm excitation, dotted lines) of mit-roGFP1 for all mitochondria in panel D. A binary mask (BIN) was calculated for each image in the time-sequence (the inset shows the BIN image at $T = 0$ s) to determine mitochondrial fluorescence signals. (F) Similar to panel C but now for mit-roGFP1. Of note, mit-roGFP1 is more oxidized than cyt-roGFP1. Used fibroblast cell line: #223V [76].

was higher in the mitochondrial matrix than in the cytosol of healthy human skin fibroblasts [76]. In agreement with previous findings in HeLa cells [75] the results in Fig. 4 demonstrate that mt-roGFP1 is initially neither fully oxidized nor fully reduced in the mitochondrial matrix of human skin fibroblasts. This means that the redox potential of these mitochondria lies within the effective range of roGFP1, allowing studies of redox changes in these cells.

4.2. Manipulation of mitochondrial ROS

Until recently, mitochondrial ROS were mostly associated with oxidative damage and pathology. However, evidence is accumulating that they can also function as regulatory molecules thus playing an important role in normal cell and organismal physiology. As already mentioned in the introduction, cellular ROS-induced damage and -signaling has often been studied using exogenous ROS generating systems that increase ROS throughout the cell ('global' ROS). However, given the physicochemical properties of the various ROS, it is likely that different ROS have a different range of action that might be limited to a small subcellular volume surrounding the site of its generation ('local' ROS; see also the section about HyPer above). Gaining a proper understanding of ROS-induced damage and -signaling therefore requires techniques that allow (combined) local detection of ROS (see previous section) and local manipulation of ROS. The amount of (local) ROS in a cell depends on the balance between: (i) its generation and (ii) its removal by antioxidants. Experimental approaches to manipulate this balance are described below.

4.2.1. Targeted pro-oxidants

4.2.1.1. Proteinaceous pro-oxidants. In principle, a genetically-encoded photosensitizer should be suited to generate ROS in different cellular compartments including mitochondria. The first example of such a photosensitizer is a red fluorescent protein derived from the non-fluorescent and non-phototoxic chromoprotein anm2CP[20] in *hydrozoa* jellyfish [78]. This modified protein, called KillerRed (KR), can be visualized in living cells using low-intensity excitation at 515–560 nm and emission detection at 555–700 nm [79]. High intensity illumination of KR at 515–560 nm will then result in photoactivation and ROS generation. Expression of KR in different mitochondria and cell compartments might be suited for studying the effects of (local) ROS generation at specific cell locations. Obviously, this is only feasible after careful investigation of possible side-effects of KR-activation (*e.g.* lipid peroxidation) and optimization of the KR photoactivation protocol. In comparison to enhanced green fluorescent protein (EGFP), KR phototoxicity is at least 1000-fold higher and its light-induced ROS production

can be used for chromophore-assisted light inactivation (CALI; [79]) of a KR-attached protein. This might for instance be applied to inactivate proteins involved in ROS homeostasis (*e.g.* SODs), provided that endogenous non-FP-labeled SODs can be largely exchanged by their over-expressed FP-coupled counterparts. Proper mitochondrial targeting of KR requires the presence of two mitochondrial targeting sequences. Unfortunately, KR forms dimers that might affect the function of KR-fused proteins. The latter can possibly be overcome by using a tandem version leading to internal dimerization of KR [79].

4.2.1.2. Cell penetrating peptides. Cell penetrating peptides (CPPs) can cross the plasma membrane and thereby introduce cargo like proteins, nucleic acids, small molecule therapeutics and fluorescent quantum dots into the cell [80]. Part of the CPPs are also mitochondria-penetrating peptides (MPPs) because they specifically accumulate in mitochondria [81]. Similar to TPP^+-linked compounds (see Section 4.2.2) currently identified MPPs have both cationic and lipophilic properties, which facilitate permeation of the MIM and mitochondrial targeting. MPPs enter the cell via a direct uptake mode thereby bypassing endocytosis and avoiding endosomal/lysosomal sequestration [81,82]. MPPs are able to deliver negatively charged and zwitterionic small molecules, but do require a certain level of lipophilicity of the cargo. A member of the MMP family, TO-FrFK, was used to study oxidative stress responses triggered by mitochondria-generated ROS in living HeLa and MRC-5 cells. TO-FrFK contains a thiazole orange (TO) moiety, which generates $^1O_2$ upon photoactivation [83].

4.2.2. Targeted antioxidants

The levels, localization and/or activities of cellular antioxidants are essential in determining which biological responses are initiated by ROS [6,12,84]. Given the importance of oxidative stress due to mitochondria-generated ROS during pathological conditions, considerable effort has been put into the development of proteinaceous and chemical compounds that reduce ROS levels and/or prevent ROS-induced damage. Use of these compounds allows site-specific blocking of (the effects of) mitochondrial ROS, but also scavenging of specific types of ROS in, for instance, rotenone- and vehicle-treated control cells [21,85]. Below we discuss some of these compounds in more detail.

4.2.2.1. Proteinaceous antioxidants. To specifically reduce mitochondrial $O_2^{\bullet-}$ and H_2O_2 levels, overexpression of the mitochondrial SOD (MnSOD) and mt-CAT has been performed [86,87]. Also CuZnSOD, that normally resides in the cytosol and the mitochondrial intermembrane space, was expressed in the mitochondrial matrix by fusing it to a mitochondrial targeting sequence [86].

4.2.2.2. TPP^+-linked chemical antioxidants. In analogy to mito-HEt (Section 4.1.1.1) and applying a concept pioneered by Skulachev et al. to investigate $\Delta\psi$ (*e.g.* [88,89]), antioxidant moieties such as CoQ or vitamin E can be targeted to the mitochondrial matrix by conjugating them to lipophilic cations like TPP^+ via an alkyl chain (see [85,90] and the references therein). A series of mitochondria-targeted antioxidants was developed to selectively decrease $O_2^{\bullet-}$ (MitoSOD), H_2O_2 (MitoPeroxidase), Fe^{2+} (MitoTEMPOL) and lipid peroxidation ($MitoQ_{10}$ and $MitoE_2$). The first TPP^+-linked compound contained the antioxidant moiety of α-tocopherol ($MitoE_2$). Here the subscript 2 indicates that the linking alkyl chain has a length of 2 carbon atoms. Structurally, $MitoE_2$ strongly resembles a TPP^+-coupled form of Trolox (6-hydroxy-2,5,7,8-tetramethylchroman-2-carboxylic acid), which is a water-soluble antioxidant derived from α-tocopherol. $MitoE_2$ proved more effective than its non-targeted variant in preventing peroxidation of mitochondrial lipids [85].

The TPP^+-linked form of CoQ ($MitoQ_{10}$) is reduced by CII, but not CI, into its active ubiquinol form. This regeneration makes $MitoQ_{10}$ a far better antioxidant than $MitoE_2$. Because MitoQ is almost entirely adsorbed into the matrix face of the inner membrane, it can prevent lipid peroxidation as was shown in isolated mitochondria. In agreement with this finding, $MitoQ_{10}$ fully prevented the rotenone-induced increase in C11-$BODIPY^{581/591}$ oxidation (*i.e.* lipid peroxidation) without affecting the rotenone-induced increase in HEt oxidation [21].

In an effort to generate stronger antioxidants, plastoquinone (a chloroplast ubiquinone) was coupled to TPP^+ [91]. When compared to CoQ, plastoquinone has methyl groups instead of methoxy groups, whereas the methyl group of CoQ is replaced by a hydrogen atom. Based upon its membrane-permeability, plastoquinonyl-decyl-TPP^+ (a.k.a. SkQ1) was selected for further research. It was reported that [SkQ1] acted as an antioxidant between 25 and 800 nM, whereas at higher concentrations it displayed pro-oxidant properties. In comparison, this range was estimated between 300 and 500 nM for $MitoQ_{10}$. The antioxidant activity of SkQ1 was regenerated in the mitochondrion and it effectively prevented peroxidation of the mitochondrial lipid cardiolipin and ROS-induced apoptosis.

4.2.2.3. Mitochondria-targeted peptides. Given their cationic nature, $MitoE_2$, $MitoQ_{10}$, SkQ1 and all other TPP^+-based antioxidants are taken up by mitochondria in a $\Delta\psi$-dependent manner. This makes them likely less efficient under conditions of (highly) depolarized $\Delta\psi$. Interestingly, a novel class of cell-permeable small peptides ('SS-peptides') with intrinsic antioxidant properties were designed, that were taken up by mitochondria in a manner that was largely $\Delta\psi$-independent [92,93]. SS-peptides are water-soluble, stable in aqueous solution, designed to resist degradation by peptidases and consist of an alternating aromatic-cationic motif with basic amino acids like arginine and lysine. SS-02 (*i.e.* Dmt-D-Arg-Phe-Lys-NH_2; Dmt = 2′,6′-dimethyltyrosine) and SS-31 (D-Arg-Dmt-Lys-Phe-NH_2) were demonstrated to localize to the MIM. Although the reason for this mitochondrial targeting is currently unknown, there might be an electrostatic interaction between the cationic peptides and the anionic MIM lipid cardiolipin. Replacement of the tyrosine residue by a phenylanaline eliminated the H_2O_2, $OH^{\bullet}$ and $ONOO^-$ scavenging activities of the SS peptide, suggesting that the phenolic tyrosine group mediates antioxidant activity. In this respect, it is already known that dimethyltyrosine is a potent scavenger of oxyradicals. It is thought that SS-02 and SS-31 prevent lipid peroxidation by scavenging of $OH^{\bullet}$ [92,93].

Another approach to specifically deliver molecules to the mitochondria involves the use of the antibacterial membrane disruptor, gramicidin S (GS). Given the similarities between bacterial membranes and the MIM, it might be possible to re-engineer GS in such a way that it becomes a mitochondria-targeting moiety to which 'cargo' compound can be attached. This is illustrated by the molecule 'XJV-5-131' [94], which contains: (i) as cargo a ROS scavenger like the stable nitroxide radical TEMPOL, and (ii) as mitochondrial targeting moiety a portion of the membrane-active portion of GS. TEMPOL undergoes redox recycling, oxidizes free iron thereby preventing Fenton reactions, and also exhibits SOD-mimetic activity [90,94]. Unfortunately, GS-based compounds can also interfere with natural redox defense mechanisms and mitochondrial respiration by reacting with antioxidants and MitoQ [95].

5. Conclusion

There is still much controversy about how different mitochondrial ROS generating systems contribute to mitochondrial/cellular ROS levels, redox signaling and oxidative damage during healthy and pathological conditions. This arises from the fact that a large amount of model systems (*e.g.* isolated proteins, individual mitochondria and intact primary or cancer cells) and experimental approaches (*e.g.* metabolic conditions, used OXPHOS inhibitors, different ways to stimulate ROS production, different reporter molecules) have been

used to investigate ROS and redox homeostasis. The complex mitochondrial physiology, in combination with the central role of these organelles in cellular survival, requires a genesis between data obtained with isolated mitochondria and living cells. Largely based upon our own practical experience, we here reviewed: (i) fluorescence microscopy techniques allowing assessment of (specific) ROS and/or its downstream consequences at the cellular and mitochondrial level, and (ii) approaches for manipulation of (specific) ROS and/or its downstream consequences. Proper analysis of ROS homeostasis in living cells requires the combined use of multiple ROS reporter molecules in parallel experiments, assessment of non-ROS-related parameters that can induce artifacts (*e.g.* $\Delta\psi$, pH) and inclusion of conditions known to affect mitochondrial ROS generation as positive and negative controls (*e.g.* OXPHOS inhibitors, mitochondrial uncoupling, O_2 depletion). To differentiate between local (mitochondrial) and global (cellular) ROS effects, results obtained with local manipulations have to be compared with those obtained using ROS generating systems and non-targeted antioxidants that affect cellular ROS levels.

Acknowledgements

This project was supported by a grant from the IGMD (Institute for Genetic and Metabolic Disease) of the Radboud University Nijmegen Medical Centre (RUNMC) to WJHK and equipment grants of ZON (Netherlands Organization for Health Research and Development, no: 903-46-176) and NWO (Netherlands Organization for Scientific Research, no: 911-02-008). We are grateful to Prof. S.J. Remington (University of Oregon, Eugene, OR, USA) for supplying the cDNA's encoding redox-sensitive green fluorescent protein 1 (roGFP1), Dr. S. Verkaart (Dept. of Physiology, RUNMC) for performing the redox measurements and Dr. A.S. De Jong (Dept. of Biochemistry, RUNMC) for the HEt and Mito-HEt experiments.

References

[1] L. Tretter, V. Adam-Vizi, Generation of reactive oxygen species in the reaction catalyzed by alpha-ketoglutarate dehydrogenase, J. Neurosci. 24 (2004) 7771–7778.
[2] A.A. Starkov, G. Fiskum, C. Chinopoulos, B.J. Lorenzo, S.E. Browne, M.S. Patel, M.F. Beal, Mitochondrial alpha-ketoglutarate dehydrogenase complex generates reactive oxygen species, J. Neurosci. 24 (2004) 7779–7788.
[3] I. Dalle-Donne, R. Rossi, D. Giustarini, R. Colombo, A. Milzani, S-glutathionylation in protein redox regulation, Free Radic. Biol. Med. 43 (2007) 883–898.
[4] W. Koopman, S. Verkaart, H. Visch, S. van Emst-de Vries, L. Nijtmans, J. Smeitink, P. Willems, Human NADH:ubiquinone oxidoreductase deficiency: radical changes in mitochondrial morphology? Am. J. Physiol. Cell Physiol. 293 (2007) C22–C29.
[5] M. Valko, D. Leibfritz, J. Moncol, M. Cronin, M. Mazur, J. Telser, Free radicals and antioxidants in normal physiological functions and human disease, Int. J. Biochem. Cell Biol. 39 (2007) 44–84.
[6] E.A. Veal, A.M. Day, B.A. Morgan, Hydrogen peroxide sensing and signaling, Mol. Cell 26 (2007) 1–14.
[7] A.A. Starkov, The role of mitochondria in reactive oxygen species metabolism and signaling, Ann. N. Y. Acad. Sci. 1147 (2008) 37–52.
[8] W.J. Koopman, L.G. Nijtmans, C.E. Dieteren, P. Roestenberg, F. Valsecchi, J.A. Smeitink, P.H. Willems, in press. Mammalian mitochondrial complex I: Biogenesis, regulation and reactive oxygen species generation, Antioxid Redox Signal. PMID: 19803744.
[9] M.C. Carreras, J.J. Poderoso, Mitochondrial nitric oxide in the signaling of cell integrated responses, Am. J. Physiol. Cell Physiol. 292 (2007) C1569–C1580.
[10] R.W. Redmond, I.E. Kochevar, Spatially resolved cellular responses to singlet oxygen, Photochem. Photobiol. 82 (2006) 1178–1186.
[11] A.V. Zima, L.A. Blatter, Redox regulation of cardiac calcium channels and transporters, Cardiovasc. Res. 71 (2006) 310–321.
[12] M. Giorgio, M. Trinei, E. Migliaccio, P. Pelicci, Hydrogen peroxide: a metabolic by-product or a common mediator of ageing signals? Nat. Rev. Mol. Cell Biol. 8 (2007) 722–728.
[13] C.C. Winterbourn, Reconciling the chemistry and biology of reactive oxygen species, Nat. Chem. Biol. 4 (2008) 278–286.
[14] V. Adam-Vizi, C. Chinopoulos, Bioenergetics and the formation of mitochondrial reactive oxygen species, Trends Pharmacol. Sci. 27 (2006) 639–645.
[15] M. Murphy, How mitochondria produce reactive oxygen species, Biochem. J. 417 (2009) 1–13.
[16] B.D. Sidell, Intracellular oxygen diffusion: the roles of myoglobin and lipid at cold body temperature, J. Exp. Biol. 201 (1998) 1119–1128.
[17] T.V. Votyakova, I.J. Reynolds, DeltaPsi(m)-dependent and -independent production of reactive oxygen species by rat brain mitochondria, J. Neurochem. 79 (2001) 266–277.
[18] Y. Liu, G. Fiskum, D. Schubert, Generation of reactive oxygen species by the mitochondrial electron transport chain, J. Neurochem. 80 (2002) 780–787.
[19] I. Sipos, L. Tretter, V. Adam-Vizi, Quantitative relationship between inhibition of respiratory complexes and formation of reactive oxygen species in isolated nerve terminals, J. Neurochem. 84 (2003) 112–118.
[20] I. Sipos, L. Tretter, V. Adam-Vizi, The production of reactive oxygen species in intact isolated nerve terminals is independent of the mitochondrial membrane potential, Neurochem. Res. 28 (2003) 1575–1581.
[21] W. Koopman, S. Verkaart, H. Visch, F. van der Westhuizen, M. Murphy, L. van den Heuvel, J. Smeitink, P. Willems, Inhibition of complex I of the electron transport chain causes O2−. -mediated mitochondrial outgrowth, Am. J. Physiol. Cell Physiol. 288 (2005) C1440–C1450.
[22] L. Tretter, V. Adam-Vizi, Moderate dependence of ROS formation on DeltaPsim in isolated brain mitochondria supported by NADH-linked substrates, Neurochem. Res. 32 (2007) 569–575.
[23] E. Cadenas, A. Boveris, C.I. Ragan, A.O. Stoppani, Production of superoxide radicals and hydrogen peroxide by NADH-ubiquinone reductase and ubiquinol–cytochrome *c* reductase from beef-heart mitochondria, Arch. Biochem. Biophys. 180 (1977) 248–257.
[24] J.F. Turrens, A. Alexandre, A.L. Lehninger, Ubisemiquinone is the electron donor for superoxide formation by complex III of heart mitochondria, Arch. Biochem. Biophys. 237 (1985) 408–414.
[25] L. Tretter, V. Adam-Vizi, Alpha-ketoglutarate dehydrogenase: a target and generator of oxidative stress, Philos. Trans. R. Soc. Lond. B Biol. Sci. 360 (2005) 2335–2345.
[26] L. Tretter, K. Takacs, V. Hegedus, V. Adam-Vizi, Characteristics of alpha-glycerophosphate-evoked H2O2 generation in brain mitochondria, J. Neurochem. 100 (2007) 650–663.
[27] L. Tretter, K. Takacs, K. Kover, V. Adam-Vizi, Stimulation of H(2)O(2) generation by calcium in brain mitochondria respiring on alpha-glycerophosphate, J. Neurosci. Res. 85 (2007) 3471–3479.
[28] M. Vrbacky, Z. Drahota, T. Mracek, A. Vojtiskova, P. Jesina, P. Stopka, J. Houstek, Respiratory chain components involved in the glycerophosphate dehydrogenase-dependent ROS production by brown adipose tissue mitochondria, Biochim. Biophys. Acta 1767 (2007) 989–997.
[29] T. Mracek, A. Pecinova, M. Vrbacky, Z. Drahota, J. Houstek, High efficiency of ROS production by glycerophosphate dehydrogenase in mammalian mitochondria, Arch. Biochem. Biophys. 481 (2009) 30–36.
[30] S.S. Korshunov, B.F. Krasnikov, M.O. Pereverzev, V.P. Skulachev, The antioxidant functions of cytochrome *c*, FEBS Lett. 462 (1999) 192–198.
[31] M.O. Pereverzev, T.V. Vygodina, A.A. Konstantinov, V.P. Skulachev, Cytochrome *c*, an ideal antioxidant, Biochem. Soc. Trans. 31 (2003) 1312–1315.
[32] A. Okado-Matsumoto, I. Fridovich, Subcellular distribution of superoxide dismutases (SOD) in rat liver: Cu,Zn-SOD in mitochondria, J. Biol. Chem. 276 (2001) 38388–38393.
[33] H.N. Kirkman, G.F. Gaetani, Mammalian catalase: a venerable enzyme with new mysteries, Trends Biochem. Sci. 32 (2007) 44–50.
[34] T.S. Chang, C.S. Cho, S. Park, S. Yu, S.W. Kang, S.G. Rhee, Peroxiredoxin III, a mitochondrion-specific peroxidase, regulates apoptotic signaling by mitochondria, J. Biol. Chem. 279 (2004) 41975–41984.
[35] Z. Cao, J.G. Lindsay, N.W. Isaacs, Mitochondrial peroxiredoxins, Subcell. Biochem. 44 (2007) 295–315.
[36] J.M. Mates, C. Perez-Gomez, I. Nunez de Castro, Antioxidant enzymes and human diseases, Clin. Biochem. 32 (1999) 595–603.
[37] R.A. Smith, C.M. Porteous, C.V. Coulter, M.P. Murphy, Selective targeting of an antioxidant to mitochondria, Eur. J. Biochem. 263 (1999) 709–716.
[38] G.W. Burton, K.U. Ingold, Vitamin E as an in vitro and in vivo antioxidant, Ann. N. Y. Acad. Sci. 570 (1989) 7–22.
[39] M. Valko, C.J. Rhodes, J. Moncol, M. Izakovic, M. Mazur, Free radicals, metals and antioxidants in oxidative stress-induced cancer, Chem. Biol. Interact. 160 (2006) 1–40.
[40] M. Bentinger, K. Brismar, G. Dallner, The antioxidant role of coenzyme Q, Mitochondrion 7 (2007) S41–S50 Suppl.
[41] K.M. Robinson, M.S. Janes, M. Pehar, J.S. Monette, M.F. Ross, T.M. Hagen, M.P. Murphy, J.S. Beckman, Selective fluorescent imaging of superoxide in vivo using ethidium-based probes, Proc. Natl. Acad. Sc.i USA 103 (2006) 15038–15043.
[42] H. Zhao, J. Joseph, H.M. Fales, E.A. Sokoloski, R.L. Levine, J. Vasquez-Vivar, B. Kalyanaraman, Detection and characterization of the product of hydroethidine and intracellular superoxide by HPLC and limitations of fluorescence, Proc. Natl. Acad. Sci. USA 102 (2005) 5727–5732.
[43] W.J. Koopman, F. Distelmaier, J.J. Esseling, J.A. Smeitink, P.H. Willems, Computer-assisted live cell analysis of mitochondrial membrane potential, morphology and calcium handling, Methods 46 (2008) 304–311.
[44] D.G. Nicholls, Simultaneous monitoring of ionophore- and inhibitor-mediated plasma and mitochondrial membrane potential changes in cultured neurons, J. Biol. Chem. 281 (2006) 14864–14874.
[45] W.J. Koopman, S. Verkaart, S.E. van Emst-de Vries, S. Grefte, J.A. Smeitink, P.H. Willems, Simultaneous quantification of oxidative stress and cell spreading using 5-(and-6)-chloromethyl-2′, 7′-dichlorofluorescein, Cytometry A 69 (2006) 1184–1192.
[46] G.E. Gibson, H. Zhang, H. Xu, L.C. Park, T.M. Jeitner, Oxidative stress increases internal calcium stores and reduces a key mitochondrial enzyme, Biochim. Biophys. Acta 1586 (2002) 177–189.
[47] W. Koopman, S. Verkaart, S. van Emst-de Vries, S. Grefte, J. Smeitink, L. Nijtmans, P. Willems, Mitigation of NADH:ubiquinone oxidoreductase deficiency by chronic Trolox treatment, Biochim. Biophys. Acta 1777 (2008) 853–859.

[48] S.L. Hempel, G.R. Buettner, Y.Q. O'Malley, D.A. Wessels, D.M. Flaherty, Dihydrofluorescein diacetate is superior for detecting intracellular oxidants: comparison with 2′, 7′-dichlorodihydrofluorescein diacetate, 5(and 6)-carboxy-2′, 7′-dichlorodihydrofluorescein diacetate, and dihydrorhodamine 123, Free Radic. Biol. Med. 27 (1999) 146–159.
[49] A. Keller, A. Mohamed, S. Drose, U. Brandt, I. Fleming, R.P. Brandes, Analysis of dichlorodihydrofluorescein and dihydrocalcein as probes for the detection of intracellular reactive oxygen species, Free Radic. Res. 38 (2004) 1257–1267.
[50] Y.Q. O'Malley, K.J. Reszka, B.E. Britigan, Direct oxidation of 2′, 7′-dichlorodihydrofluorescein by pyocyanin and other redox-active compounds independent of reactive oxygen species production, Free Radic. Biol. Med. 36 (2004) 90–100.
[51] D.A. Bass, J.W. Parce, L.R. Dechatelet, P. Szejda, M.C. Seeds, M. Thomas, Flow cytometric studies of oxidative product formation by neutrophils: a graded response to membrane stimulation, J. Immunol. 130 (1983) 1910–1917.
[52] P. Wardman, Fluorescent and luminescent probes for measurement of oxidative and nitrosative species in cells and tissues: progress, pitfalls, and prospects, Free Radic. Biol. Med. 43 (2007) 995–1022.
[53] E. Marchesi, C. Rota, Y.C. Fann, C.F. Chignell, R.P. Mason, Photoreduction of the fluorescent dye 2′-7′-dichlorofluorescein: a spin trapping and direct electron spin resonance study with implications for oxidative stress measurements, Free Radic. Biol. Med. 26 (1999) 148–161.
[54] C.L. Murrant, M.B. Reid, Detection of reactive oxygen and reactive nitrogen species in skeletal muscle, Microsc. Res. Tech. 55 (2001) 236–248.
[55] A. Gomes, E. Fernandes, J.L. Lima, Fluorescence probes used for detection of reactive oxygen species, J. Biochem. Biophys. Methods 65 (2005) 45–80.
[56] G. Drummen, L. van Liebergen, J. Op den Kamp, J. Post, C11-BODIPY(581/591), an oxidation-sensitive fluorescent lipid peroxidation probe: (micro)spectroscopic characterization and validation of methodology, Free Radic. Biol. Med. 33 (2002) 473–490.
[57] E.H. Pap, G.P. Drummen, V.J. Winter, T.W. Kooij, P. Rijken, K.W. Wirtz, J.A. Op den Kamp, W.J. Hage, J.A. Post, Ratio-fluorescence microscopy of lipid oxidation in living cells using C11-BODIPY(581/591), FEBS Lett. 453 (1999) 278–282.
[58] J. Lippincott-Schwartz, E. Snapp, A. Kenworthy, Studying protein dynamics in living cells, Nat. Rev. Mol. Cell Biol. 2 (2001) 444–456.
[59] S.B. VanEngelenburg, A.E. Palmer, Fluorescent biosensors of protein function, Curr. Opin. Chem. Biol. 12 (2008) 60–65.
[60] L. Filippin, M.C. Abad, S. Gastaldello, P.J. Magalhaes, D. Sandona, T. Pozzan, Improved strategies for the delivery of GFP-based Ca2+ sensors into the mitochondrial matrix, Cell Calcium 37 (2005) 129–136.
[61] A.E. Palmer, M. Giacomello, T. Kortemme, S.A. Hires, V. Lev-Ram, D. Baker, R.Y. Tsien, Ca2+ indicators based on computationally redesigned calmodulin–peptide pairs, Chem. Biol. 13 (2006) 521–530.
[62] A. Miyawaki, A. Sawano, T. Kogure, Lighting up cells: labelling proteins with fluorophores, Nat. Cell Biol. (2003) S1–S7 (Suppl).
[63] T. Kogure, H. Kawano, Y. Abe, A. Miyawaki, Fluorescence imaging using a fluorescent protein with a large Stokes shift, Methods 45 (2008) 223–226.
[64] T. Nagai, A. Sawano, E.S. Park, A. Miyawaki, Circularly permuted green fluorescent proteins engineered to sense Ca2+, Proc. Natl. Acad. Sci. USA 98 (2001) 3197–3202.
[65] W. Wang, H. Fang, L. Groom, A. Cheng, W. Zhang, J. Liu, X. Wang, K. Li, P. Han, M. Zheng, J. Yin, M.P. Mattson, J.P. Kao, E.G. Lakatta, S.S. Sheu, K. Ouyang, J. Chen, R.T. Dirksen, H. Cheng, Superoxide flashes in single mitochondria, Cell 134 (2008) 279–290.
[66] F.L. Muller, A critical evaluation of cpYFP as a probe for superoxide, Free Radic. Biol. Med. 47 (2009) 1779–1780.
[67] M. Willemse, E. Janssen, F. de Lange, B. Wieringa, J. Fransen, ATP and FRET—a cautionary note, Nat. Biotechnol. 25 (2007) 170–172.
[68] V.V. Belousov, A.F. Fradkov, K.A. Lukyanov, D.B. Staroverov, K.S. Shakhbazov, A.V. Terskikh, S. Lukyanov, Genetically encoded fluorescent indicator for intracellular hydrogen peroxide, Nat. Methods 3 (2006) 281–286.
[69] G. Miesenbock, D.A. De Angelis, J.E. Rothman, Visualizing secretion and synaptic transmission with pH-sensitive green fluorescent proteins, Nature 394 (1998) 192–195.
[70] A. Esposito, M. Gralle, M.A. Dani, D. Lange, F.S. Wouters, pHlameleons: a family of FRET-based protein sensors for quantitative pH imaging, Biochemistry 47 (2008) 13115–13126.
[71] K. Markvicheva, E. Bogdanova, D. Staroverov, S. Lukyanov, V. Belousov, Imaging of intracellular hydrogen peroxide production with HyPer upon stimulation of HeLa cells with epidermal growth factor, Methods Mol. Biol. 476 (2009) 76–83.
[72] A. Espinosa, A. Garcia, S. Hartel, C. Hidalgo, E. Jaimovich, NADPH oxidase and hydrogen peroxide mediate insulin-induced calcium increase in skeletal muscle cells, J. Biol. Chem. 284 (2009) 2568–2575.
[73] Z.I. Ungvari, N. Labinskyy, P. Mukhopadhyay, J.T. Pinto, Z. Bagi, P. Ballabh, C. Zhang, P. Pacher, A. Csiszar, Resveratrol attenuates mitochondrial oxidative stress in coronary arterial endothelial cells, Am. J. Physiol. Heart Circ. Physiol. 297 (2009) H1876–H1881.
[74] P. Niethammer, C. Grabher, A.T. Look, T.J. Mitchison, A tissue-scale gradient of hydrogen peroxide mediates rapid wound detection in zebrafish, Nature 459 (2009) 996–999.
[75] G.T. Hanson, R. Aggeler, D. Oglesbee, M. Cannon, R.A. Capaldi, R.Y. Tsien, S.J. Remington, Investigating mitochondrial redox potential with redox-sensitive green fluorescent protein indicators, J. Biol. Chem. 279 (2004) 13044–13053.
[76] S. Verkaart, W. Koopman, J. Cheek, S. van Emst-de Vries, L. van den Heuvel, J. Smeitink, P. Willems, Mitochondrial and cytosolic thiol redox state are not detectably altered in isolated human NADH:ubiquinone oxidoreductase deficiency, Biochim. Biophys. Acta 1772 (2007) 1041–1051.
[77] C.T. Dooley, T.M. Dore, G.T. Hanson, W.C. Jackson, S.J. Remington, R.Y. Tsien, Imaging dynamic redox changes in mammalian cells with green fluorescent protein indicators, J. Biol. Chem. 279 (2004) 22284–22293.
[78] M.E. Bulina, D.M. Chudakov, O.V. Britanova, Y.G. Yanushevich, D.B. Staroverov, T.V. Chepurnykh, E.M. Merzlyak, M.A. Shkrob, S. Lukyanov, K.A. Lukyanov, A genetically encoded photosensitizer, Nat. Biotechnol. 24 (2006) 95–99.
[79] M.E. Bulina, K.A. Lukyanov, O.V. Britanova, D. Onichtchouk, S. Lukyanov, D.M. Chudakov, Chromophore-assisted light inactivation (CALI) using the phototoxic fluorescent protein KillerRed, Nat. Protoc. 1 (2006) 947–953.
[80] S.B. Fonseca, M.P. Pereira, S.O. Kelley, Recent advances in the use of cell-penetrating peptides for medical and biological applications, Adv. Drug Deliv. Rev. 61 (2009) 953–964.
[81] K.L. Horton, K.M. Stewart, S.B. Fonseca, Q. Guo, S.O. Kelley, Mitochondria-penetrating peptides, Chem. Biol. 15 (2008) 375–382.
[82] L.F. Yousif, K.M. Stewart, K.L. Horton, S.O. Kelley, Mitochondria-penetrating peptides: sequence effects and model cargo transport, Chembiochem 10 (2009) 2081–2088.
[83] K.P. Mahon, T.B. Potocky, D. Blair, M.D. Roy, K.M. Stewart, T.C. Chiles, S.O. Kelley, Deconvolution of the cellular oxidative stress response with organelle-specific peptide conjugates, Chem. Biol. 14 (2007) 923–930.
[84] B. D'Autreaux, M.B. Toledano, ROS as signalling molecules: mechanisms that generate specificity in ROS homeostasis, Nat. Rev. Mol. Cell Biol. 8 (2007) 813–824.
[85] M. Murphy, R. Smith, Targeting antioxidants to mitochondria by conjugation to lipophilic cations, Annu. Rev. Pharmacol. Toxicol. 47 (2007) 629–656.
[86] M.W. Epperly, J.E. Gretton, C.A. Sikora, M. Jefferson, M. Bernarding, S. Nie, J.S. Greenberger, Mitochondrial localization of superoxide dismutase is required for decreasing radiation-induced cellular damage, Radiat. Res. 160 (2003) 568–578.
[87] M.W. Epperly, J.A. Melendez, X. Zhang, S. Nie, L. Pearce, J. Peterson, D. Franicola, T. Dixon, B.A. Greenberger, P. Komanduri, H. Wang, J.S. Greenberger, Mitochondrial targeting of a catalase transgene product by plasmid liposomes increases radioresistance in vitro and in vivo, Radiat. Res. 171 (2009) 588–595.
[88] L.E. Bakeeva, L.L. Grinius, A.A. Jasaitis, V.V. Kuliene, D.O. Levitsky, E.A. Liberman, I.I. Severina, V.P. Skulachev, Conversion of biomembrane-produced energy into electric form. II. Intact mitochondria, Biochim. Biophys. Acta 216 (1970) 13–21.
[89] E.A. Liberman, V.P. Skulachev, Conversion of biomembrane-produced energy into electric form. IV. General discussion, Biochim. Biophys. Acta 216 (1970) 30–42.
[90] V.E. Kagan, P. Wipf, D. Stoyanovsky, J.S. Greenberger, G. Borisenko, N.A. Belikova, N. Yanamala, A.K. Samhan Arias, M.A. Tungekar, J. Jiang, Y.Y. Tyurina, J. Ji, J. Klein-Seetharaman, B.R. Pitt, A.A. Shvedova, H. Bayir, Mitochondrial targeting of electron scavenging antioxidants: regulation of selective oxidation vs random chain reactions, Adv. Drug Deliv. Rev. (2009).
[91] V. Skulachev, V. Anisimov, Y. Antonenko, L. Bakeeva, B. Chernyak, V. Erichev, O. Filenko, N. Kalinina, V. Kapelko, N. Kolosova, B. Kopnin, G. Korshunova, M. Lichinitser, L. Obukhova, E. Pasyukova, O. Pisarenko, V. Roginsky, E. Ruuge, I.I. Senin, I.I. Severina, M. Skulachev, I. Spivak, V. Tashlitsky, V. Tkachuk, M. Vyssokikh, L. Yaguzhinsky, D. Zorov, An attempt to prevent senescence: a mitochondrial approach, Biochim. Biophys. Acta 1787 (2009) 437–461.
[92] H.H. Szeto, Development of mitochondria-targeted aromatic-cationic peptides for neurodegenerative diseases, Ann. N. Y. Acad. Sci. 1147 (2008) 112–121.
[93] H.H. Szeto, Mitochondria-targeted cytoprotective peptides for ischemia–reperfusion injury, Antioxid. Redox Signal. 10 (2008) 601–619.
[94] M.P. Fink, C.A. Macias, J. Xiao, Y.Y. Tyurina, R.L. Delude, J.S. Greenberger, V.E. Kagan, P. Wipf, Hemigramicidin-TEMPO conjugates: novel mitochondria-targeted antioxidants, Crit. Care Med. 35 (2007) S461–S467.
[95] J. Trnka, F. Blaikie, R. Smith, M. Murphy, A mitochondria-targeted nitroxide is reduced to its hydroxylamine by ubiquinol in mitochondria, Free Radic. Biol. Med. 44 (2008) 1406–1419.